

# Motif-based Convolutional Neural Network on Graphs

Aravind Sankar<sup>†\*</sup>, Xinyang Zhang<sup>‡\*</sup>, Kevin Chen-Chuan Chang<sup>†</sup>

<sup>†</sup>Department of Computer Science, University of Illinois at Urbana-Champaign, USA

<sup>‡</sup> Department of Computer Science and Technology, Tsinghua University, China  
{asankar3, kcchang}@illinois.edu, zhangxinyang14@mails.tsinghua.edu.cn

## Abstract

This paper introduces a generalization of Convolutional Neural Networks (CNNs) from regular grid-structured data such as images to graphs with irregular linkage structures, especially expressive heterogeneous graphs with typed nodes and schemas. We propose a novel spatial convolution operation to model the key aspects of a CNN: local connectivity and translation invariance, using higher-order structures. We use the concept of *motif*, which provides us flexibility to describe spatial locality in Heterogeneous graphs with respect to its schema, or any graph with respect to desired higher-order connection patterns. We develop a novel neural network architecture *Motif-CNN* that captures higher-order structural and feature information by combining the information extracted from multiple patterns through deeper layers. Our experiments on semi-supervised learning tasks on social networks and real-world heterogeneous graphs indicate significant gains over existing graph CNNs and respective state-of-the-art techniques.

## 1 Introduction

CNNs (LeCun et al. 1998) have achieved immense success in various machine learning tasks where the underlying data representation is grid-structured, such as image classification, object detection and speech processing (LeCun, Bengio, and Hinton 2015). Their efficacy has inspired researchers to explore the CNN paradigm in non-euclidean domains such as Natural Language (Kim 2014), Graphs (Bruna et al. 2014) and Manifolds (Masci et al. 2015).

Two fundamental properties of the input data utilized in the design of CNNs are *local connectivity* and *translation invariance*. The neurons in a CNN extract features from small localized regions in the data, known as local receptive fields and share parameters across different spatial locations thus capturing translation invariance. This enables them to significantly reduce the number of parameters without sacrificing the ability to extract informative patterns from the data.

In many scenarios, we encounter data lying in irregular domains that can be naturally represented as graphs encoding rich interactions between various real-world entities. For instance, an academic citation network (such as DBLP) is composed of multiple types of nodes, viz. authors, papers

and venues inter-connected in different relationships. Such heterogeneous graphs are typically associated with a schema that specifies the type of nodes and their allowable connection patterns.

Direct generalizations of CNNs to graphs is non-trivial since real-world graphs do not share the same locality patterns as in grid-structured data. For example, convolutional filter design in images directly follows from the structure of the data manifold where every pixel has eight neighbors with precise spatial locations. Graphs however possess irregular neighborhood structures with varying number of neighbors per node, that renders standard notions of locality and translation inapplicable. Furthermore, most modern graphs are heterogeneous, comprising nodes of several types with diverse feature sets, which necessitates fine-grained modeling of interactions between different types subject to the schema and domain semantics.

The key challenge in designing an effective convolution operation lies in identifying the structural properties of the data that are vital to capturing relevant features. We outline two key objectives or requirements for an effective spatial CNN on graphs:

**R1** Definition of spatial locality that identifies the local receptive field around a node, subject to the diversity of node types, semantics and heterogeneous interactions.

**R2** Design of a weight-sharing mechanism such that two nodes share the same weight in two different locations of the receptive field if and only if their structural roles (position within the receptive field) are identical.

Though the requirements outlined above seem natural, existing graph CNNs fall short of addressing them satisfactorily. Recent work on graph CNNs fall into two categories: spectral and spatial. Spectral techniques focus on defining convolution using an inner product in the Fourier domain, while spatial techniques define convolution through weight-sharing among local neighborhoods of the graph.

Spectral CNNs employ the analogy between classic Fourier transforms and projection onto the eigenbasis of the graph Laplacian to define filters as spectral multipliers on the eigenvectors of the Laplacian (Henaff, Bruna, and LeCun 2015). To define localized spectral filters in the vertex domain, recent techniques have designed parameterized filters such as cubic splines and Chebychev polynomials (Bruna et al. 2014; Defferrard, Bresson, and Vandergheynst 2016). In

\*Equal contribution

all of these methods, the learned spectral filters are functions of the Laplacian eigenbasis which is unique for each graph, i.e. a spectral CNN learnt on one graph cannot be applied to another graph with a different structure, thus severely limiting applicability in most real-world scenarios.

On the other hand, spatial CNNs define *spatial locality* (R1) based on neighborhood proximity i.e. immediate neighbors of each node, which is insufficient to discover the structural properties and semantics of many real-world networks. For example, higher-order structures such as triangles are strongly indicative of community structure in social networks (Holland and Leinhardt 1970), which otherwise may not be evident. This becomes even more apparent in heterogeneous graphs since not every pair of nodes can connect (e.g., in DBLP, an author does not link to another author; they connect through a paper). In such a scenario, the locality around an author can be described in various ways, such as by her co-authors, her published venues, etc., each carrying different semantics. A type-agnostic view of locality would fail to capture such rich interactions between nodes of different types. Thus, defining an appropriate notion of spatial locality, subject to graph heterogeneity is the **first key challenge** in designing an effective graph CNN.

Weight-sharing mechanisms (R2) proposed by existing spatial CNNs fail to sufficiently differentiate the structural roles of nodes in the local receptive field and do not generalize to expressive heterogeneous graphs with schemas. Existing schemes explore weight-sharing by: hop distance from a node (Atwood and Towsley 2016), linearizing the neighborhood through a canonical ordering (Niepert, Ahmed, and Kutzkov 2016), or aggregation of immediate neighborhood (Duvenaud et al. 2015; Kipf and Welling 2017; Such et al. 2017). While all these methods extract local features around a node, they lack the capability to incorporate the semantics of real-world graphs in modeling the structural roles of various nodes in the neighborhood, which is critical to designing an effective convolution operation. Thus, we identify the clear delineation of the structural roles of nodes in the receptive field as our **second key challenge**.

**Present work:** In this work, we develop a generic flexible graph CNN that is applicable on both homogeneous and heterogeneous graphs. We briefly describe how our model addresses the challenges outlined above.

First, we model the local receptive field around a target node of interest using the concept of *motifs*. Motifs, also known as higher-order structures are small subgraph patterns with a specific connections among different node types and as repeatedly found (e.g., (Milo et al. 2002; Benson, Gleich, and Leskovec 2016)) are fundamental building blocks of large and complex networks. Recent research has explored higher-order analysis of graphs using motifs in various applications such as graph clustering (Benson, Gleich, and Leskovec 2016), community search (Huang et al. 2014), strong tie detection (Rotabi et al. 2017), etc. We exploit motifs to describe the context around a target node thus capturing higher-order semantics of interactions in real-world graphs.

Second, we present a formal definition of motifs that delineates the structural roles of context nodes in the receptive

	Dimensions	Description
$N$	Scalar	# nodes
$D$	Scalar	# input features/channels
$F$	Scalar	# filters learnt per motif
$K_M$	Scalar	# unique structural roles in motif $M$
$U$	Scalar	# motifs/Conv. units in one Convolutional Layer
$X$	$N \times D$	Input Feature Matrix
$H_l^j$	$N \times F$	Activations at Conv unit $j$ (motif $M_j$ ) in layer $l$
$\mathcal{A}^M$	$K_M \times N \times N$	Motif-Adjacency tensor for motif $M$
$W^M$	$(K_M + 1) \times D \times F$	Filter weight tensor for motif $M$

Table 1: Notations

field and define a novel spatial convolution operation that extracts features across motif instances in the local neighborhood. To the best of our knowledge, we are the first to explore the concept of motifs for graph convolution.

Finally, we propose a novel CNN architecture *Motif-CNN* that enables the use of multiple motif patterns concurrently to learn higher-order features capturing rich interactions through deeper layers. *Motif-CNN* seamlessly generalizes to graphs of diverse domains by allowing a user to provide as input semantically meaningful patterns relevant to the task.

We conduct experiments on two semi-supervised learning (SSL) tasks on multiple real-world datasets. Our experimental results on classification in Social Networks and heterogeneous graphs, and clustering in Ego-Networks demonstrate the effectiveness of our model in leveraging higher-order features through motifs.

## 2 Preliminaries

In this section, we introduce some notations that will be used throughout the paper. A Graph is defined as  $G = (V, E)$  with node type mapping  $l : V \mapsto \mathcal{L}$  where  $V = \{v_1, \dots, v_N\}$  is a finite set of  $N$  nodes,  $E$  is the set of edges and  $\mathcal{L}$  is the node type set. Heterogeneous graphs often have a schema to express the allowable links between different node types. Note that the above definition can be trivially generalized to include link types, but we exclude them for the sake of brevity.

The nodes are collectively described by a feature matrix  $X \in \mathbb{R}^{N \times D}$  where  $D$  is the number of features/channels. Since nodes of different types in a heterogeneous graph can potentially belong to different feature spaces, we concatenate the feature representations of different node types (with zero padding) to obtain a joint representation of  $D$  channels. We assume a small set of  $U$  domain-specific motifs given by  $U_M = \{M_1, \dots, M_U\}$  as input. Our goal is to learn a graph convolutional network that serves as a prediction model on the nodes of the graph given task-specific supervision.

## 3 Graph Convolutional Neural Network

Our objective is to design a flexible CNN for graphs that can generalize to diverse applications and effectively utilize domain-specific patterns. We revisit the key properties of a CNN to motivate the formulation of our graph convolutional model. A conventional CNN models the context of a pixel (local receptive field) using a ‘square-grid’ of fixed

size and extracts *translationally invariant* features by scanning a square filter across the grid-structured input. In the scenario of graphs, the goal of a CNN is to model the information at a specific node of interest - *target* node using features extracted from neighboring nodes - *context* nodes.

The first step towards defining convolution on graphs is the concept of **local connectivity**. Let us revisit DBLP, with the goal of predicting the research area of an author. Though an author is linked only to papers, the venues and citations of her published papers provide strong cues in identifying her research area. It is thus necessary to look beyond the immediate neighbors to model local connectivity through higher-order structures. We use *motif*, a higher-order structure that encodes a linkage pattern among nodes of various types, to model spatial locality for a specific node type. In Fig. 1(a), motif  $M_1$  is a pattern that describes the locality around a target author  $A$  through context nodes  $P_1, P_2$  and  $V_3$ . Here, we use lower-case letters (e.g.,  $a$ ) to denote nodes in  $G$  and upper-case letters (e.g.,  $A$ ) to denote node types. In Fig. 1(a), the subscript under a context node gives the node index, for e.g.,  $P_1$  and  $P_2$  are two different nodes of type  $P$ . An author node  $a$  is now characterized via different instances of motif  $M_1$  in  $G$  with  $a$  as target (illustrated in Fig. 1(b)), i.e.  $a$  is locally connected with the context nodes in the two marked instances. We formalize this notion by using a motif to define a local receptive field specific to a node type.

The second step is to define the concept of **translation invariance** in graphs to achieve weight-sharing across local neighborhoods. In Fig. 1(b),  $a_1$  and  $a_2$  are connected to target node  $a$  via motif  $M_3$  and represent co-authors who are expected to share a similar relationship with  $a$ . Generalizing this idea, we posit that the context nodes linked via certain patterns of connections share the same *structural roles* relative to the target node. Since a motif contains multiple context nodes, it is essential to delineate the *structural roles* of each context node to accurately model weight-sharing. In motif  $M_2$  (Fig. 1(a)), it is evident that the roles of  $P_1, P_2$  and  $V_3$  relative to target  $A$  are quite different, while the roles of  $P_1$  and  $P_2$  are indistinguishable in motif  $M_1$ . For instance, nodes  $p_1$  and  $p_2$  share the same structural role relative to target node  $a$  in the marked instance of  $M_1$  (Fig. 1(b)). Thus, two context nodes in the local receptive field share the same structural roles in motif  $M$  if and only if they belong to the same type and are structurally symmetric relative to the target node. The structural roles are defined specific to a motif and hence the number of unique roles  $K_M$  is bounded by the number of context nodes.

### 3.1 Graph Motif

Conventionally, a motif (or metagraph) has been defined as a pattern of edges among different node types (Benson, Gleich, and Leskovec 2016; Fang et al. 2016). Such a definition does not model the locality around a specific node type which is our primary objective here. Hence, we propose a novel definition of motifs that clearly identifies the local receptive field around a node (of a given type) and demarcates the structural roles of different context nodes. We define a graph motif  $M$  as a subgraph composed of a designated *target* node  $t_M$  and a relevant subset of *context* nodes, where

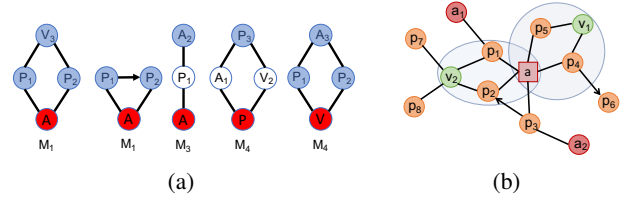


Figure 1: (a) Sample Motifs in DBLP - Types: Author (A), Paper (P) and Venue (V) with target in red and context in blue (b) Example graph with instances of  $M_1$  for target  $a$ .

the role of each context node is determined by the type and structural symmetry relative to  $t_M$ . Formally, we describe a motif as below:

**Definition 1:** A motif  $M$  with target  $t_M$  and context nodes  $C_M$  is defined as  $M = (V_M, E_M, C_M, t_M)$  with node type mapping  $l_M : V_M \mapsto \mathcal{L}$  where  $V_M$  is a set of nodes with  $t_M \in V_M$  and  $C_M \subseteq V_M - \{t_M\}$ ,  $E_M$  is a set of edges and  $\forall x \in V_M, l_M(x) \in \mathcal{L}$ .

We define an instance  $S_u$  of motif  $M$  with target node  $u$  in  $G$  as a subgraph induced by  $M$  with  $u$  as the designated target node.

The formal definition of an instance is given by:

**Definition 2:** An instance  $S_u = (V_S, E_S)$  of motif  $M$  with target node  $u$  on  $G$  is a subgraph of  $G$  where  $V_S$  is a set of nodes and  $E_S$  is a set of edges, such that there exists a bijection  $\psi_S : V_S \mapsto V_M$  satisfying (i)  $u \in V_S$ ,  $\psi_S(u) = t_M$  (ii)  $\forall x \in V_S, l(x) = l_M(\psi_S(x))$  and (iii)  $\forall x, y \in V_S, (x, y) \in E_S$  if  $(\psi_S(x), \psi_S(y)) \in E_M$ .

The local receptive field around a target node is defined by the structure of motif  $M$ . The set of all instances of  $M$  in  $G$  with target node  $u$  denoted by  $I_u^M$ , constitute the region spanned by the local receptive field (motif  $M$ ) around target  $u$ . In homogeneous graphs, the local receptive field defined by a motif is potentially applicable on all nodes.

The structural roles of context nodes w.r.t target  $u$  in an instance  $S_u \in I_u^M$  can be easily deduced from the structure and types of nodes in  $M$ . The number of unique structural roles in  $M$  is given by  $K_M (< |C_M|)$ . Thus, we denote  $\phi(V_S, E_S, u, c)$ , a role mapping function that takes an instance  $S_u = (V_S, E_S)$ , target  $u \in V_S$ , context  $c \in V_S$  and returns the structural role ( $\in \{1, \dots, K_M\}$ ) of  $c$  relative to  $u$ .

### 3.2 Convolutional Unit

In this section, we propose a novel spatial convolution operation to extract local features for a specific type of node, using a local receptive field described by motif  $M$ . Specifically, given a motif  $M$  with target node type  $T \in \mathcal{L}$ , we describe motif-based convolution for nodes in the graph of type  $T$ .

We define a motif *filter* as a set of weights over the  $K_M$  unique structural roles of context nodes in  $M$ . Given a target node  $v_i \in V$  with  $l(v_i) = T$  and motif  $M$  as input, we describe the convolution operation at node  $v_i$ . For ease of explanation, we restrict our initial definitions to a single channel ( $D = 1$ ) and single filter per motif ( $F = 1$ ).

**Motif Filter:** A motif filter (on  $M$ ) is defined by a weight

$w_0$  for target  $t_M$  and a weight vector  $\mathbf{w} \in \mathbb{R}^{K_M}$  for the  $K_M$  context roles. Each role  $k$  in  $M$  is associated with a corresponding weight in  $\mathbf{w}$  to differentiate the structural roles of surrounding context nodes in the local receptive field.

Before describing our convolution operation, we first introduce a few notations to describe role-specific node connectivity via motifs.

**Motif-adjacency Tensor:** We define a motif-adjacency tensor to encode the occurrences of nodes in each unique structural role over all instances in the graph. We denote by  $\mathcal{A}^M$ , a tensor of  $K_M$  matrices, that encodes the connectivity of nodes through  $M$  in each role  $k$ .  $\mathcal{A}_{kij}^M$  is the number of times context node  $v_j$  appeared in an instance of  $M$  in role  $k$  with  $v_i$  as target. Formally,

$$\mathcal{A}_{kij}^M = \sum_{S_{v_i} \in I_{v_i}^M} I(\phi(V_S, E_S, v_i, v_j) = k)$$

where  $I(\cdot)$  is the indicator function. We also define a diagonal matrix  $\mathcal{D}^M \in \mathbb{R}^{N \times N}$  to store the number of motif instances at each node (as target), i.e.  $\mathcal{D}_{ii}^M = L_i \forall i \leq N$ .

**Motif-based convolution:** To define convolution at node  $v_i$ , the features of all nodes that are locally connected through motif  $M$  are weighted based on their structural roles, normalized by the diagonal matrix that reduces the bias introduced by highly connected nodes. Convolution at node  $v_i$  via motif  $M$  is given as :

$$h^M(v_i) = \sigma \left( w_0 x_i + \frac{1}{\mathcal{D}_{ii}^M} \sum_{j=1}^N \sum_{k=1}^{K_M} w_k \mathcal{A}_{kij}^M x_j \right) \quad (1)$$

where  $x_i$  and  $x_j$  refer to the features of nodes  $v_i$  and  $v_j$  respectively,  $h^M(v_i)$  is the output of convolution at node  $v_i$  and  $\sigma(\cdot)$  is an activation function, such as  $\text{ReLU}(\cdot) = \max(0, \cdot)$ .

From Eqn. 1, it is evident that weight-sharing is achieved by assigning the same weight to context nodes that share the same structural role relative to  $v_i$  across all instances of motif  $M$  containing  $v_i$ . We term this operation as a *convolutional unit* (Conv unit) for motif  $M$ .

We generalize Eqn. 1 for input  $X \in \mathbb{R}^{N \times D}$  with  $N$  nodes,  $D$  channels and  $F$  filters per motif. The output of a Conv unit (for motif  $M$ ) is expressed as,

$$H^M = \sigma \left( X W_0^M + (\mathcal{D}^M)^{-1} \sum_{k=1}^{K_M} \mathcal{A}_k^M X W_k^M \right) \quad (2)$$

$W^M \in \mathbb{R}^{(K_M+1) \times D \times F}$  is a tensor of filter parameters for motif  $M$  and  $H^M \in \mathbb{R}^{N \times F}$  is the output of the Conv unit. To summarize, a Conv unit defined on motif  $M$  extracts features from nodes connected through the motif  $M$ , weights them based on their roles and applies a non-linear activation.

### 3.3 Architecture of Motif-CNN

So far, we have described a Conv unit that performs convolution over the local neighborhood of a target node using a single motif  $M$  to obtain a first-order feature map. However, the end goal (as is the case for any CNN) of a graph CNN is to learn global higher-order features through deeper layers. Unlike traditional convolutional filters that extract features around each pixel in an image, a motif filter models the locality only for certain nodes in the graph. For instance, a

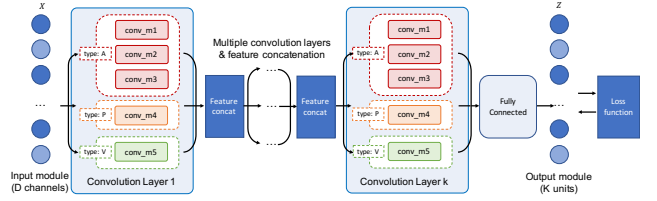


Figure 2: Architecture of *Motif-CNN* for motifs in Fig. 1(a)

triangular motif can model the context around densely connected nodes in a community but would fail to extract features for nodes with only one neighbor. Furthermore, a motif cannot be applied to every node in the graph since nodes may have different types. Thus, it is essential to leverage information from multiple relevant motifs for effective feature learning. To this end, we propose a deep architecture *Motif-CNN* that uses multiple Conv units (each corresponding to a motif) in each convolutional layer.

In order to facilitate higher-order feature learning, the features learnt for a node in one layer must serve as input (as context) to other nodes in the next layer. Since a single motif extracts features only for specific nodes in the graph, it is necessary to incorporate the features learnt via different motifs to effectively propagate information through deeper layers. To achieve this, we concatenate the feature maps obtained from different motifs and provide that as the input to the next convolutional layer. Fig. 2 illustrates the architecture of *Motif-CNN* for the motifs shown in Fig. 1(a).

The architecture comprises multiple stacked convolutional layers to enable higher-order feature learning via non-linear interactions between different motifs, followed by a fully connected layer. Let  $U$  denote the number of Conv units in one layer. The output of Conv unit  $j$  at layer  $l$  is given by  $H_l^j$  (Eqn. 2). The output at the  $l$ -th convolutional layer is denoted by  $H_l$ , with  $H_0 = X$ .  $H_l$  is obtained through feature concatenation, i.e.  $H_l = [H_l^1, \dots, H_l^U]$ . The output module and loss function depend on the prediction task. We consider two SSL tasks:

**Semi-supervised node classification:** Classify nodes into  $K$  classes given a small set of labeled examples in each class. The output module has  $K$  units and applies the softmax activation function to obtain  $Z \in \mathbb{R}^{N \times K}$ . We use a cross-entropy loss function given by,

$$L = - \sum_{l \in Y_L} \sum_{k=1}^K Y_{lk} \log Z_{lk} \quad (3)$$

where  $Y_L$  is the set of node indices that have labels. For multi-label classification, we use  $K$  sigmoid units in the output module and apply the binary cross-entropy loss function.

**Semi-supervised clustering:** Cluster nodes given a set of pairwise constraints indicating that a pair of nodes belong to the same cluster. We employ a graph-based loss function on the output representations of each node as below,

$$L = \sum_{(u,v) \in Y_L} -\log \sigma(\mathbf{z}_u^T \mathbf{z}_v) - \sum_{q=1}^Q \log E_{v_n \sim P_n} \log \sigma(-\mathbf{z}_u^T \mathbf{z}_{v_n}) \quad (4)$$

where  $Y_L$  is the set of pairwise constraints,  $Q$  is the number of negative samples and  $P_n$  is a negative sampling distribu-

tion (similar to (Perozzi, Al-Rfou, and Skiena 2014)). For every pair  $(u, v)$  that belongs to the same cluster, we include both  $(u, v)$  and  $(v, u)$  in  $Y_L$  since pairwise constraints are symmetric. Finally, we use  $k$ -means to cluster nodes based on their output representations.

### 3.4 Complexity analysis and implementation

The space complexity depends on the number of motifs  $U$  (typically  $< 5$ ) and the density of each  $\mathcal{A}^M$ , given by  $O(U|\mathcal{A}_{avg}^M|)$ . In practice, the average number of context roles in a motif ( $K_{avg}$ ) is  $\leq 3$  and the role-specific matrices are sparser than the original adjacency matrix, giving an average-case space complexity  $O(UK_{avg}|E|)$ . Next, we describe the details of computing motif-specific adjacency tensors, that were introduced in the previous section.

**Computation of Motif-Adjacency Tensor:** The motif-adjacency tensor provides a representation of role-specific connectivity via motifs, that is both compact and allows pre-computation. A simple strategy is to employ subgraph matching to enumerate all instances of motif  $M$  in  $G$ , thus populating the entries of the tensor. Though efficient parallel algorithms for subgraph matching enable reasonable computation times for motifs of size  $\leq 5$ , we adopt a different strategy for computing this tensor.

We observe that in most motifs (all motifs in our experiments), the set of paths linking the context and target nodes are independent and cover all nodes. This enables us to express the role-specific connectivity matrices using a combination of path-based simple matrix operations. Concretely, let us take an example of motif  $M_1$  in Fig. 1(a) with target  $A$  and two context roles ( $P_1$  or  $P_2$ ) and  $V_3$ . The role-specific connectivity matrix  $\mathcal{A}_k^M$  can be given using type-specific adjacency matrices  $R_{T_i T_j}$  for types  $T_i$  and  $T_j$ . Specifically for motif  $M_1$ ,  $\mathcal{A}_0^M(P_1 \text{ or } P_2) = R_{AP} \odot (R_{AP} \cdot R_{PV} \cdot R_{PV}^T)$  and  $\mathcal{A}_1^M(V_3) = M(M > 1)$  where  $M = R_{AP} \cdot R_{PV}$  where  $\odot$  is the Hadamard product and  $M > x$  returns the indices in  $M$  where the entry is  $> x$ .

Thus, the complexity of computing the tensor is  $O(|E_M|)$  matrix operations for a single role, and an overall complexity of  $O(K_M|E_M|)$  matrix operations for a motif  $M$  with  $K_M$  roles. As evidenced in our experiments, the cost of pre-computing the tensor is negligible in most real-world graphs. In practice, not limited to  $M_1$  in Fig. 1(a), all the motifs used in our experiments can be computed by two operations (Hadamard product and multiplication) on the corresponding matrices. We find that such motifs are sufficient to capture the semantics of most heterogeneous graph schemas, nevertheless subgraph matching can be used in case of more complex interaction patterns.

**Implementation:** We provide an efficient GPU-based implementation in Tensorflow (Abadi et al. 2016) using sparse-dense matrix operations, which will be made available soon.

### 3.5 Interpretation of motif-based convolution using standard convolutions

In this section, we demonstrate that our motif-based convolution (described in Eqn. 1) can be expressed as *standard* convolution over motif instances followed by mean pooling.

Dataset	$ V $	$ E $	$D$	Classes
Flickr	13,696	1,354,461	1000	10
LinkedIn	7124	39,649	2394	3

Table 2: Statistics of Flickr and LinkedIn social networks

Recall that a conventional CNN (such as images) scans a *square* filter over all patches in the local neighborhood to extract features by computing an inner product between the filter parameters and features. Similarly, we interpret the *motif* filter as scanning the local neighborhood of a target node through its motif instances and apply the standard definition of convolution for each motif instance. Using the same notations from Sec. 3.2, we describe the *standard* convolution operation at node  $v_i$  and motif  $M$  for each motif instance  $S_{v_i} = (V_S, E_S) \in I_{v_i}^M$  by:

$$h_s^M(v_i) = w_0 x_i + \sum_{\substack{v_j \in V_S - \{v_i\} \\ \psi_S(v_j) \in C_M}} w_{\phi(V_S, E_S, v_i, v_j)} x_j \quad \forall S_{v_i} \in I_{v_i}^M \quad (5)$$

where  $h_s^M(v_i)$  is the output of convolution for instance  $s$  at node  $v_i$ . Note that only the subset of relevant context nodes are considered for convolution. This operation gives an output of convolution for each motif instance in  $I_M(v_i)$ .

Now, we can define a pooling operation to aggregate the outputs of convolution similar to traditional CNN architectures. In the specific case of applying mean pooling, we get:

$$\begin{aligned} h_{new}^M(v_i) &= \sigma \left( \text{pool} \left( \{h_s^M(v_i) : S_{v_i} \in I_{v_i}^M\} \right) \right) = \sigma \left( \frac{1}{L_i} \sum_{s=1}^{L_i} h_s^M(v_i) \right) \\ &= \sigma \left( w_0 x_i + \frac{1}{L_i} \sum_{s=1}^{L_i} \sum_{\substack{v_j \in V_S - \{v_i\} \\ \psi_S(v_j) \in C_M}} w_{\phi(V_S, E_S, v_i, v_j)} x_j \right) \end{aligned} \quad (6)$$

where  $h_{new}^M(v_i)$  is the output at node  $v_i$  after pooling. On observing Eqn. 6 carefully, we can express the second term as a sum over each node  $v_j$  in  $G$  weighted by the occurrence count of  $v_j$  in the context of target  $v_i$  in role  $k$ , thus giving:

$$h_{new}^M(v_i) = \sigma \left( w_0 x_i + \frac{1}{D_{ii}^M} \sum_{j=1}^N \sum_{k=1}^{K_M} w_k \mathcal{A}_{kij}^M x_j \right)$$

We can clearly observe the equivalence of the above expression with Eqn. 1, thus providing an interpretation of standard convolution over motif instances, followed by a mean pooling aggregation. This provides a strong basis for our motif-based formulation, since it generalizes primitives of conventional convolution and pooling operations to graphs. It is also instructive to note that in case of using simply an “edge” as a motif, our model (Eqn. 2) approximately reduces to that of GCN (Kipf and Welling 2017). Thus, it is evident that *Motif-CNN* generalizes state-of-the-art graph convolutional networks through higher-order structures or motifs.

## 4 Experiments

In this section, we present experiments on homogeneous and heterogeneous graph datasets. In both settings, we compare against two graph CNN methods a) GCN (Kipf and Welling 2017) and b) DCNN (Atwood and Towsley 2016).

Dataset	$ V $	$ E $	$D$	$ G $	$K$
Facebook	3959	168,486	224	10	120
Twitter	52,665	885,520	1110	565	2223

Table 3: Statistics of Ego-networks:  $|G|$ : Number of ego-networks,  $K$ : Number of clusters

We exclude other spectral methods since they have already been shown inferior to GCN. Since our model is applicable on various tasks, we provide a comprehensive evaluation by comparing against multiple state-of-the-art task-specific baselines, in addition to existing Graph CNN methods.

#### 4.1 Homogeneous Graphs

We conduct experiments on Social Network datasets with node attributes on two tasks: Semi-supervised classification and Semi-supervised clustering.

**Semi-supervised classification:** We use two real-world social media datasets obtained from Flickr<sup>1</sup> and LinkedIn (Li, Wang, and Chang 2014) in our experiments. In Flickr, the graph is described by the friendship network among users, node attributes by user interest tags and classes by user interest groups. LinkedIn is a set of ego-networks with node attributes given by user profiles and classes by tags assigned by the ego-user to his friends into various categories, such as classmates, colleagues, etc. We only include ego-networks with at least 10% labeled nodes per class in our experiments. Flickr corresponds to a multi-label scenario, while LinkedIn is multi-class. Table. 2 illustrates the dataset statistics.

**Experimental setup:** In each dataset, we randomly sample 20% of the labeled examples for training, 10% for validation and the rest for testing. We repeat this process 10 times, and report the average performance in terms of both Micro- $F_1$  and Macro- $F_1$ . Unless otherwise stated, we train a 3-layer *Motif-CNN* with ReLU activations and tune hyperparameters (learning rate, dropout rate and number of filters per motif) based on the validation set. We train all graph CNNs for a maximum of 200 epochs using Adam (Kingma and Ba 2014) with windowed early stopping on the validation set. Since we expect motifs such as triangles to be discriminative in social networks, we experiment with  $\Delta$  and ( $\Delta + edge$ ) as patterns.

**Baselines:** Additionally, we compare against two standard baselines for SSL on graphs:

- ICA: Iterative classification algorithm that uses local and relational features for node classification (Sen et al. 2008).
- Planetoid: SSL framework based on graph embeddings (Yang, Cohen, and Salakhudinov 2016)

**Experimental results:** We summarize the classification results in Table. 4. We observe that *Motif-CNN* ( $\Delta + edge$ ) outperforms other benchmark algorithms and achieves gains of 5% in Flickr and 9% in LinkedIn (Macro- $F_1$ ) over the next-best method. *Motif-CNN* ( $\Delta$ ) suffers from sparsity for nodes of low-degree, which is offset by *Motif-CNN*

<sup>1</sup><https://www.flickr.com/>

Method	Flickr		LinkedIn	
	Micro- $F_1$	Macro- $F_1$	Micro- $F_1$	Macro- $F_1$
DCNN	46.39	46.96	70.27	54.81
GCN	41.71	42.24	71.91	57.53
Planetoid	31.53	31.39	62.49	43.63
ICA	28.53	22.45	63.39	47.55
Motif-CNN ( $\Delta$ )	47.05	47.45	72.13	58.75
Motif-CNN ( $\Delta + edge$ )	<b>48.52</b>	<b>49.59</b>	<b>73.13</b>	<b>62.90</b>

Table 4: Classification results on Flickr and LinkedIn.

Method	Facebook		Twitter	
	Jaccard	F1	Jaccard	F1
DCNN	0.390	0.497	0.292	0.406
GCN	0.381	0.496	0.322	0.446
CESNA	0.329	0.435	0.329	0.392
Motif-SC ( $\Delta$ )	0.316	0.437	0.316	0.380
LSGR	0.349	0.455	0.298	0.414
Motif-CNN ( $\Delta$ )	0.413	0.524	0.322	0.446
Motif-CNN ( $edge + \Delta$ )	<b>0.418</b>	<b>0.528</b>	<b>0.353</b>	<b>0.479</b>

Table 5: Clustering results on Ego-network datasets with 5% pairwise constraints

( $\Delta + edge$ ) that uses both edge and triangle patterns simultaneously. This demonstrates the ability of *Motif-CNN* to learn feature associations through triangle patterns that are important in social networks. Other methods such as ICA and Planetoid model node features independent of the graph structure, which leads to their poor performance.

**Semi-supervised clustering:** We evaluate our model on ego-networks obtained from Facebook and Twitter<sup>2</sup>. Ground-truth clusters are given by overlapping social circles (or ‘lists’ in Twitter), and the node attributes come from user profiles (or hashtags in twitter). We exclude clusters with less than 5 nodes and include only those networks with at least 2 clusters. Table. 3 details the dataset statistics. We train all Graph CNNs using the same loss function (Eqn. 4).

**Baselines:** Additionally, we compare against the following state-of-the-art techniques for clustering:

- **CESNA:** An unsupervised generative model to detect overlapping communities (Yang, McAuley, and Leskovec 2013). We use it as a standard benchmark for comparison.
- **Motif-SC:** An unsupervised motif-spectral clustering algorithm (Benson, Gleich, and Leskovec 2016).
- **LSGR:** Semi-supervised graph clustering framework that uses pair-wise constraints (Yang et al. 2015).

We quantify performance using two widely used metrics for overlapping community detection: Jaccard similarity and  $F_1$  score (Yang, McAuley, and Leskovec 2013).

**Experimental results:** Table. 5 compares the performance of different methods at 5% pairwise constraints. We observe relative gains of 6% and 7% in  $F_1$  score on Facebook

<sup>2</sup><http://snap.stanford.edu/data>

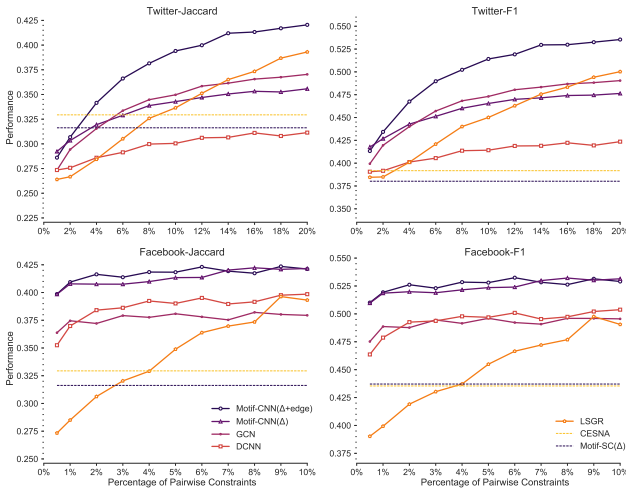


Figure 3: Clustering results on Facebook and Twitter

and Twitter datasets respectively. Fig. 3 illustrates the variation in performance of the methods with increasing percentage of pair-wise constraints. In Facebook, we find that *Motif-CNN* ( $\Delta+edge$ ) outperforms other baselines significantly, while *Motif-CNN* ( $\Delta$ ) is also comparable. In Twitter, *Motif-CNN* ( $\Delta$ ) does not perform well since the ego-networks are quite sparse with  $\sim 20\%$  of nodes having in/out degree less than 2 on average, however *Motif-CNN* ( $\Delta+edge$ ) alleviates this problem and beats other methods significantly. In Facebook, convergence is achieved with just 2% constraints while 10-15% constraints are necessary in Twitter. Overall, *Motif-CNN* significantly outperforms other methods, which indicates the effectiveness of capturing interactions via triangle patterns along with node features for social-circle detection.

## 4.2 Heterogeneous Graphs

We conduct classification experiments on heterogeneous graphs using three real-world datasets (statistics in Table. 6):

- **DBLP-A:** This is a bibliographic citation graph composed of 3 node types: author ( $A$ ), paper ( $P$ ) and venue ( $V$ ), connected by three link types:  $P \rightarrow P$ ,  $A \rightarrow P$  and  $P \rightarrow V$ . We use a subset of DBLP (Sun et al. 2011) with text features of papers to classify authors based on their research areas.
- **DBLP-P:** This dataset has the same schema as DBLP, but the task is to classify research papers. The categories of papers are extracted from Cora (McCallum et al. 2000).
- **Movie:** We use MovieLens (Harper and Konstan 2016) to create a graph with 4 node types: movie ( $M$ ), user ( $U$ ), actor ( $A$ ) and tag ( $T$ ) linked by 4 types:  $U \rightarrow M$ ,  $A \rightarrow M$ ,  $U \rightarrow T$  and  $M \rightarrow T$ , with features available for actors and movies, for movie genre prediction which is multi-label classification.

**Experimental setup:** We sample 10% of the labeled examples for training, 10% for validation and rest for testing. For node types that do not have features, we assume 1-hot encoded inputs for the Graph convolutional models. For

Dataset	$ V $	$ E $	$ \mathcal{L} $	Classes
DBLP-A	11,170	24,846	3	4
DBLP-P	35,770	131,636	3	10
Movie	10,441	99,509	4	6

Table 6: Statistics of heterogeneous graph datasets

*Motif-CNN*, we first enumerate a small set of relevant motif patterns with  $|V_M| \leq 4$  based on the schema of the Heterogeneous graph. Then, we choose the best subset of patterns for our final experiments based on validation set performance. We have made these details available online<sup>3</sup>.

**Baselines:** We also compare our model with multiple strong baselines designed for SSL on heterogeneous graphs:

- **LP-Metapath:** An SSL algorithm that utilizes metapath-specific Laplacians to jointly propagate labels and learn weights for different metapaths (Wan et al. 2015).
- **LP-Metagraph:** State-of-the-art SSL algorithm on heterogeneous graphs based on an ensemble of Metagraph guided random walks (Jiang et al. 2017).
- **Column Network (CLN):** Deep neural network for classification in multi-relational graphs (Pham et al. 2017).
- **HCC:** Collective classification method that exploits dependencies based on multiple metapaths (Kong et al. 2012).
- **metapath2vec:** A heterogeneous skip-gram model that learns node embeddings via metapath-based random walks (Dong, Chawla, and Swami 2017).

For metapath-based methods, we provide all relevant metapaths and for LP-Metagraph, we use all Metagraphs with  $\leq 4$  nodes and report the best performance among their three ensemble methods. Note that LP-Metapath and LP-Metagraph are not applicable for multi-label classification.

**Experimental results:** From Table. 7, we observe that *Motif-CNN* achieves gains of 6% and 25% (Macro- $F_1$ ) over other graph CNN models while gaining 3% and 9% overall in DBLP-A and DBLP-P respectively. Since venues are the most discriminative features in DBLP-A, simple methods based on metapaths do quite well. In DBLP-P, the features of papers and their citations are more informative, hence feature-based methods such as GCN and CLN perform better while DCNN does not scale since it has a space complexity of  $O(N^2)$  with dense matrix implementation. In the movie dataset, *Motif-CNN* performs the best (gain of 14% Macro- $F_1$  and 13% Micro- $F_1$  over graph CNN models) which can be attributed to joint modeling of structural and feature information through patterns involving users, tags and movies. Thus, we find *Motif-CNN* to convincingly outperform all graph CNN models on Heterogeneous graph datasets, while achieving similar or better performance over other state-of-art Heterogeneous classification methods.

**Running time:** The runtime of *Motif-CNN* scales with the density of the motif-adjacency tensors, similar to space complexity (see Sec. 3.4). Our experiments on homogeneous

<sup>3</sup><https://sites.google.com/site/motifcnn/>

Method	DBLP-A		DBLP-P		Movie	
	Mic-F1	Mac-F1	Mic-F1	Mac-F1	Mic-F1	Mac-F1
DCNN	69.68	69.20	x	x	49.91	46.72
GCN	81.34	81.29	71.30	53.14	55.67	53.85
LP-Metapath	82.77	82.86	62.15	52.41	-	-
LP-Metagraph	83.03	83.11	62.97	57.08	-	-
CLN	80.99	80.94	66.71	52.19	57.11	47.71
HCC	61.62	59.75	61.56	58.12	53.38	26.25
metapath2vec	83.37	83.43	70.10	61.89	60.00	60.00
Motif-CNN	<b>86.11</b>	<b>86.12</b>	<b>74.07</b>	<b>67.16</b>	<b>63.18</b>	<b>61.45</b>

Table 7: Classification results on DBLP-A, DBLP-P and Movie, - indicates *not applicable*, x indicates *does not scale*.

graphs involved  $\leq 2$  motif patterns, which yield a runtime similar to GCN. On Movie, *Motif-CNN* takes 1.33 secs per epoch with 5 motifs (typical setting) while GCN and DCNN take 0.24 secs and 7.39 secs per epoch respectively on an Intel(R) Xeon(R) CPU E5345 system with 16 GB memory. We present additional experiments in Supplementary Material.

## 5 Related Work

We organize related work in three sections: First, we briefly discuss existing work on Graph CNNs, then survey the use of motifs and finally discuss techniques relevant to various applications of our model.

**Graph CNNs:** CNNs on graphs have been explored in two general directions: spectral and spatial.

*Spectral:* These methods define convolution through the Fourier Transform described by eigenvectors of the Graph Laplacian (Bruna et al. 2014; Defferrard, Bresson, and Vandergheynst 2016). As noted in Sec. 1, spectral CNNs cannot be transferred across different graphs. Kipf and Welling propose a first-order approximation to arrive at a layer-wise linear model, thus offering a spatial interpretation.

*Spatial:* In contrast, spatial methods attempt to directly generalize convolution in the graph domain (Atwood and Towsley 2016; Niepert, Ahmed, and Kutzkov 2016; Such et al. 2017). As discussed in Sec. 1, all these methods define convolution based on just neighborhood proximity and are thus limited to learning just a single type of filter through convolution. Due to this reason, such techniques do not perform well on heterogeneous graphs that contain rich semantics of node and link types. Instead, we exploit higher-order structures through motifs to capture a richer notion of locality that naturally generalizes to heterogeneous graphs.

**Graph Motifs:** Motifs are higher-order structures that are crucial in many domains such as neuroscience (Sporns and Kötter 2004), bioinformatics (Pržulj 2007; Sankar, Ranu, and Raman 2017) and social networks. Recent works have explored motifs in clustering (Benson, Gleich, and Leskovec 2016) and strong tie detection (Rotabi et al. 2017). Motifs have also been utilized to analyze complex networks through motif-role fingerprints (McDonnell et al. 2014). On the contrary, we employ motifs to characterize the structural roles of various nodes in the context of a target node to define graph

convolution.

**Applications:** In this paper, we experiment on two SSL tasks on graphs - node classification and clustering. Graph-based SSL has been well-studied for homogeneous graphs and is often termed Collective Classification (Sen et al. 2008) when node features are used. Semi-supervised clustering (Yang et al. 2015) is a related problem that typically uses a small set of pair-wise constraints as guidance. Our model *Motif-CNN* provides a generic framework that is applicable on any graph-based SSL task.

In heterogeneous graphs, Metapaths (Wan et al. 2015) and Metagraphs (Fang et al. 2016) model pairwise node similarity, later used in downstream tasks such as classification (Jiang et al. 2017; Kong et al. 2012). Recent advances include heterogeneous skip-gram (Dong, Chawla, and Swami 2017) and deep learning models (Pham et al. 2017) for heterogeneous graphs. All these techniques use metapaths or metagraphs to model just the similarity between a pair of nodes of the same type but cannot utilize the features of all node types for classification. In contrast, we propose a unified framework to extract local features around a node through higher-order structural patterns and learn complex features through deeper layers.

## 6 Limitations and Future Work

In this section, we discuss a few limitations of *Motif-CNN* and outline directions for future work:

*Memory requirement:* This is a function of the motifs used and scales linearly with the density of  $\mathcal{A}^M$ . *Motif-CNN* is trained using full-batch gradient descent and hence cannot scale to very large graphs. An important direction for future work is to develop a mini-batch version that can approximate motif-based neighborhoods.

*Motif selection:* *Motif-CNN* assumes a small set of relevant motif patterns as input. Since the number of possible patterns is exponential in theory, an interesting direction would be to develop algorithms that can identify candidate motifs. Such techniques can particularly be useful in graphs that lack a priori domain knowledge on relevant motifs.

## 7 Conclusion

In this paper, we have introduced a novel graph CNN that captures the key aspects of local connectivity and translation invariance using the concept of motifs to define graph convolution. We presented a deep architecture that uses multiple patterns concurrently to learn higher-order features through deeper layers. Finally, we demonstrated that our approach outperforms other graph CNNs and application-specific state-of-the-art algorithms in semi-supervised classification and clustering tasks on multiple real-world datasets.

## References

- Abadi, M.; Agarwal, A.; Barham, P.; Brevdo, E.; Chen, Z.; Citro, C.; Corrado, G. S.; Davis, A.; Dean, J.; Devin, M.; et al. 2016. Tensorflow: Large-scale machine learning on heterogeneous distributed systems. *arXiv preprint arXiv:1603.04467*.
- Atwood, J., and Towsley, D. 2016. Diffusion-convolutional neural networks. In *Advances in Neural Information Processing Systems*, 1993–2001.

- Benson, A. R.; Gleich, D. F.; and Leskovec, J. 2016. Higher-order organization of complex networks. *Science* 353(6295):163–166.
- Bruna, J.; Zaremba, W.; Szlam, A.; and Lecun, Y. 2014. Spectral networks and locally connected networks on graphs. In *International Conference on Learning Representations (ICLR2014), CBLS, April 2014*.
- Defferrard, M.; Bresson, X.; and Vandergheynst, P. 2016. Convolutional neural networks on graphs with fast localized spectral filtering. In *Advances in Neural Information Processing Systems*, 3844–3852.
- Dong, Y.; Chawla, N. V.; and Swami, A. 2017. metapath2vec: Scalable representation learning for heterogeneous networks. In *Proceedings of the 23rd ACM SIGKDD International Conference on Knowledge Discovery and Data Mining*, 135–144. ACM.
- Duvenaud, D. K.; Maclaurin, D.; Iparraguirre, J.; Bombarell, R.; Hirzel, T.; Aspuru-Guzik, A.; and Adams, R. P. 2015. Convolutional networks on graphs for learning molecular fingerprints. In *Advances in neural information processing systems*, 2224–2232.
- Fang, Y.; Lin, W.; Zheng, V. W.; Wu, M.; Chang, K. C.-C.; and Li, X.-L. 2016. Semantic proximity search on graphs with metagraph-based learning. In *Data Engineering (ICDE), 2016 IEEE 32nd International Conference on*, 277–288. IEEE.
- Harper, F. M., and Konstan, J. A. 2016. The movielens datasets: History and context. *ACM Transactions on Interactive Intelligent Systems (TiiS)* 5(4):19.
- Henaff, M.; Bruna, J.; and LeCun, Y. 2015. Deep convolutional networks on graph-structured data. *CoRR* abs/1506.05163.
- Holland, P. W., and Leinhardt, S. 1970. A method for detecting structure in sociometric data. *American Journal of Sociology* 76(3):492–513.
- Huang, X.; Cheng, H.; Qin, L.; Tian, W.; and Yu, J. X. 2014. Querying k-truss community in large and dynamic graphs. In *Proceedings of the 2014 ACM SIGMOD international conference on Management of data*, 1311–1322. ACM.
- Jiang, H.; Song, Y.; Wang, C.; Zhang, M.; and Sun, Y. 2017. Semi-supervised learning over heterogeneous information networks by ensemble of meta-graph guided random walks. *IJCAI*.
- Kim, Y. 2014. Convolutional neural networks for sentence classification. In *EMNLP*, 1746–1751.
- Kingma, D. P., and Ba, J. 2014. Adam: A method for stochastic optimization. In *Proceedings of the 3rd International Conference on Learning Representations (ICLR)*.
- Kipf, T. N., and Welling, M. 2017. Semi-supervised classification with graph convolutional networks. In *International Conference for Learning Representations (ICLR 2017)*.
- Kong, X.; Yu, P. S.; Ding, Y.; and Wild, D. J. 2012. Meta path-based collective classification in heterogeneous information networks. In *Proceedings of the 21st ACM international conference on Information and knowledge management*, 1567–1571. ACM.
- LeCun, Y.; Bengio, Y.; and Hinton, G. E. 2015. Deep learning. *Nature* 521(7553):436–444.
- LeCun, Y.; Bottou, L.; Bengio, Y.; and Haffner, P. 1998. Gradient-based learning applied to document recognition. In *Proceedings of the IEEE*, volume 86, 2278–2324.
- Li, R.; Wang, C.; and Chang, K. C.-C. 2014. User profiling in an ego network: co-profiling attributes and relationships. In *Proceedings of the 23rd international conference on World wide web*, 819–830. ACM.
- Masci, J.; Boscaini, D.; Bronstein, M.; and Vandergheynst, P. 2015. Geodesic convolutional neural networks on riemannian manifolds. In *Proceedings of the IEEE international conference on computer vision workshops*, 37–45.
- McCallum, A.; Nigam, K.; Rennie, J.; and Seymore, K. 2000. Automating the construction of internet portals with machine learning. *Information Retrieval Journal* 3:127–163.
- McDonnell, M. D.; Yaveroğlu, Ö. N.; Schmerl, B. A.; Iannella, N.; and Ward, L. M. 2014. Motif-role-fingerprints: the building-blocks of motifs, clustering-coefficients and transitivity in directed networks. *PLoS one* 9(12):e114503.
- Milo, R.; Shen-Orr, S.; Itzkovitz, S.; Kashtan, N.; Chklovskii, D.; and Alon, U. 2002. Network motifs: Simple building blocks of complex networks. *Science* 298(5594):824–827.
- Niepert, M.; Ahmed, M.; and Kutzkov, K. 2016. Learning convolutional neural networks for graphs. In *International Conference on Machine Learning*, 2014–2023.
- Perozzi, B.; Al-Rfou, R.; and Skiena, S. 2014. Deepwalk: On-line learning of social representations. In *Proceedings of the 20th ACM SIGKDD international conference on Knowledge discovery and data mining*, 701–710. ACM.
- Pham, T.; Tran, T.; Phung, D. Q.; and Venkatesh, S. 2017. Column networks for collective classification. In *AAAI*, 2485–2491.
- Pržulj, N. 2007. Biological network comparison using graphlet degree distribution. *Bioinformatics* 23(2):e177–e183.
- Rotabi, R.; Kamath, K.; Kleinberg, J. M.; and Sharma, A. 2017. Detecting strong ties using network motifs. In *Proceedings of the 26th International Conference on World Wide Web Companion, Perth, Australia, April 3-7, 2017*, 983–992.
- Sankar, A.; Ranu, S.; and Raman, K. 2017. Predicting novel metabolic pathways through subgraph mining. *Bioinformatics* btx481.
- Sen, P.; Namata, G.; Bilgic, M.; Getoor, L.; Galligher, B.; and Eliassi-Rad, T. 2008. Collective classification in network data. *AI magazine* 29(3):93.
- Sporns, O., and Kötter, R. 2004. Motifs in brain networks. *PLoS biology* 2(11):e369.
- Such, F. P.; Sah, S.; Dominguez, M.; Pillai, S.; Zhang, C.; Michael, A.; Cahill, N.; and Ptucha, R. 2017. Robust spatial filtering with graph convolutional neural networks. *arXiv preprint arXiv:1703.00792*.
- Sun, Y.; Han, J.; Yan, X.; Yu, P. S.; and Wu, T. 2011. Pathsim: Meta path-based top-k similarity search in heterogeneous information networks. *Proceedings of the VLDB Endowment* 4(11):992–1003.
- Wan, M.; Ouyang, Y.; Kaplan, L.; and Han, J. 2015. Graph regularized meta-path based transductive regression in heterogeneous information network. In *Proceedings of the 2015 SIAM International Conference on Data Mining*, 918–926. SIAM.
- Yang, L.; Cao, X.; Jin, D.; Wang, X.; and Meng, D. 2015. A unified semi-supervised community detection framework using latent space graph regularization. *IEEE transactions on cybernetics* 45(11):2585–2598.
- Yang, Z.; Cohen, W.; and Salakhudinov, R. 2016. Revisiting semi-supervised learning with graph embeddings. In *International Conference on Machine Learning*, 40–48.
- Yang, J.; McAuley, J.; and Leskovec, J. 2013. Community detection in networks with node attributes. In *Data Mining (ICDM), 2013 IEEE 13th international conference on*, 1151–1156. IEEE.

## Appendix

In this section, we present a few additional experiments on the running time, and convergence of *Motif-CNN*.

### Running Time

Our experiments on homogeneous graphs typically involve  $\leq 3$  motif patterns, which yield a running time similar to GCN (Kipf and Welling 2017) - the most efficient state-of-the-art Graph Convolution technique. Hence, we do not report these numbers here.

On heterogeneous graphs, a larger number of motifs is typically necessary to capture the semantics of different node types. Hence, we investigate the influence of number of motifs used in *Motif-CNN* on the running time. We measure the running time per epoch as a function of the number of motifs ( $U$ ) input to the model. Since the running time depends on the exact motifs used and not just the number of motifs, we first enumerate a small set of relevant motif patterns with  $|V_M| \leq 4$  based on the heterogeneous graph schema and report the mean running time (with standard deviation) across all possible combinations for a fixed number of motifs.

Our experiments were performed on an 8-core x64 machine with Intel(R) Xeon(R) CPU E5345 (2.33GHz) processor and 16 GB of memory. In these experiments, we use three convolution layers with the same loss function and hyper-parameter settings (i.e. learning rate, dropout rate, hidden layer configuration etc.) for both *Motif-CNN* and GCN (Kipf and Welling 2017), while a 3-hop setting is used for DCNN (Atwood and Towsley 2016).

Fig. 4 illustrates the mean running time along with the standard deviation, on varying  $U$  (number of motifs) from 1 to 10, on DBLP-A, DBLP-P and Movie datasets. We also depict the running times of GCN and DCNN in Fig. 4 for clear comparison.

We observe from Fig. 4 that *Motif-CNN* achieves comparable running times to GCN (Kipf and Welling 2017) for a small number of motifs, while it is significantly faster in comparison to DCNN (Atwood and Towsley 2016) even when 10 motifs are used, which is quite rare. DCNN does not scale on DBLP-P due to memory limitations.

From Fig. 4, it is observed that the running time scales roughly linearly with the number of motifs input to the model, which is expected. The variance in the running time is higher in DBLP-A than in DBLP-P and Movie datasets. This is because the number of venues in the DBLP-A dataset is small ( $\sim 20$ ) which leads to patterns involving venue nodes to be much denser in comparison to others. Though we have not presented the memory consumption of *Motif-CNN*, we find that it scales with the number of motifs used, similar to the running time plots illustrated earlier (Fig. 4). A memory requirement of 16 GB is sufficient to experiment with 10 motif patterns concurrently, which is generally sufficient for all real-world datasets. Typically, we require less than 5 patterns to achieve best performance.

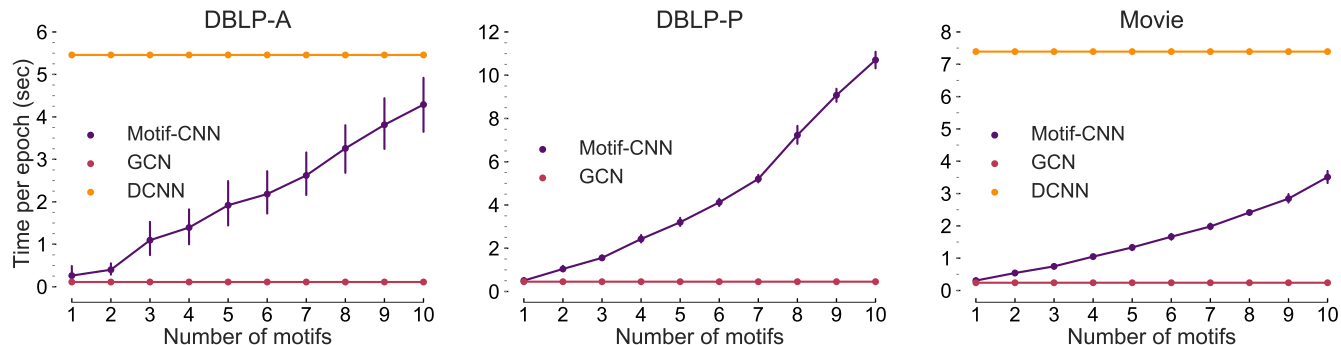


Figure 4: Running Time per epoch on varying the number of motifs ( $U$ ) in *Motif-CNN* on three Heterogeneous graph datasets DBLP-A, DBLP-P and Movie. For each value of  $U$ , the mean running time is reported, along with the standard deviation. Running times of GCN and DCNN are also illustrated for comparison.

### Convergence

We investigate the convergence of *Motif-CNN* on the heterogeneous graph datasets in comparison to existing graph CNN techniques GCN and DCNN. We use the best-configuration of motif patterns for *Motif-CNN* in this experiment. We train all models for 200 epochs with the same settings as described above and observe the convergence of validation loss w.r.t training epochs.

Fig. 5 illustrates the convergence rates of the three graph CNN methods. Since DCNN does not scale on DBLP-P due to  $O(N^2)$  complexity, we exclude it in this experiment. We find that *Motif-CNN* achieves rapid convergence in comparison to GCN and DCNN since it leverages multiple relevant patterns simultaneously. In practice, *Motif-CNN* takes similar time in total as GCN, even though it is slower per epoch, as illustrated earlier.

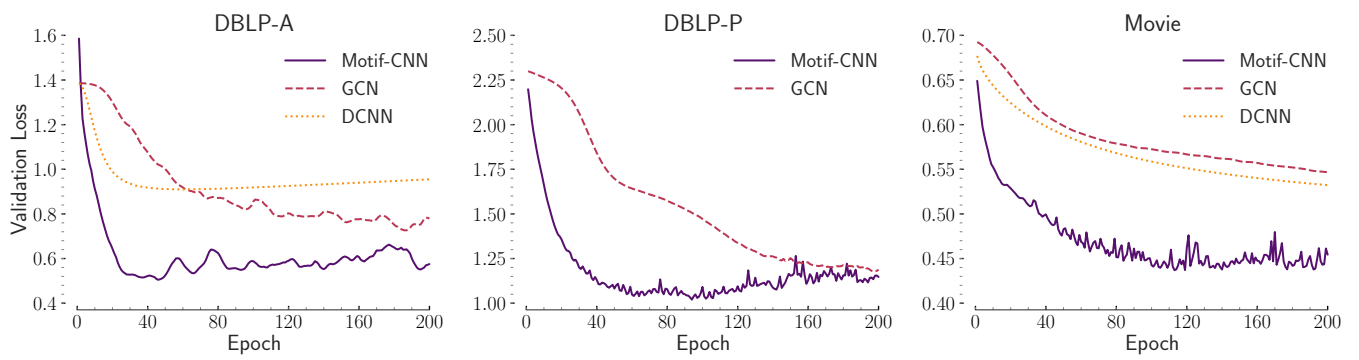


Figure 5: Convergence plots depicting validation loss w.r.t training epochs for three Graph CNN methods - GCN, DCNN and *Motif-CNN* on three Heterogeneous graph datasets DBLP-A, DBLP-P and Movie.